Nanomechanical properties of reversed surfactant bilayers formed in micrometre-sized holes†

Jian Jin,[a] Yukihiro Sugiyama,[b] Keita Mitsui,[a] Hideo Arakawa[a] and Izumi Ichinose*[a]

Received (in Cambridge, UK) 12th November 2007, Accepted 18th December 2007
First published as an Advance Article on the web 14th January 2008
DOI: 10.1039/b717485c

Nanomechanical properties of free-standing reversed surfactant bilayers, dried foam films (DFFs), were examined *via* AFM by fitting local force–indentation curves with a Hertzian model. The Young's moduli of four kinds of bilayers were in a range of 10–30 MPa.

The mechanical properties of materials of nanometre dimensions have recently attracted much attention. The properties of inorganic materials including nanotubes, nanowires, and thin films have been widely investigated in relation to sensors, nanoelectronics and micro/nano-electromechanical systems.[1–4] On the other hand, organic and organic–inorganic composite free-standing thin films have advantages in the flexibility as well as the versatility of the molecular functions.[5–8] Investigation of their mechanical properties has also been very active in recent years.[9–12] Atomic force microscopy (AFM) has been used for the nanomechanical characterization of thin polymer films on solid substrates.[13,14] The technique has also been applied to free-standing films of a few tens of nanometres.[11,15] Very recently, Jaeger and co-workers examined free-standing monolayers of close-packed gold nanoparticles modified with dodecanethiol.[16] They were surprisingly robust with the elastic modulus of 3–39 GPa despite the thickness of 9.4 nm.

We have reported that free-standing reversed bilayers of surfactant remain after drying droplets of the surfactant solution captured in micrometre-sized holes.[17] We named such bilayers "dried foam films" (DFFs), since the structure was same as foam films without an interstitial water layer. These films were stable even under ultrahigh vacuum conditions and at temperature higher than 100 °C. Very recently, we reported that silicon, carbon, and other metals and semiconductors could be deposited on DFFs by various deposition techniques.[17] This will open the door for applications such as sensing, catalysis and separation. However, their mechanical properties have remained unclear. The question is why such reversed surfactant bilayers with a thickness of a few nanometres are so stable. The objectives of the present paper are to characterize the structures of DFFs by AFM and to evaluate their nanomechanical properties. Here, we report unexpectedly high stiffness of free-standing reversed bilayers as well as their structures and thermal properties.

A TEM microgrid with a regular array of circular holes was vertically dipped into an 8.2 mM aqueous solution of dodecylphosphocholine (DPC) and dried in air. By this procedure, a small volume of the solution is captured in each hole, then two Gibbs monolayers formed at the air–water interfaces come close to each other during drying, and finally a surfactant bilayer with a head-to-head arrangement of the hydrophilic parts remains in each hole. Fig. 1A and 1B show SEM images of the DPC films covering the micrometre-sized holes. The films were not stable to the electron beam irradiation. Therefore, a 2 nm-thick platinum layer was deposited on one side of the films before observation. It is apparent that DPC films uniformly cover all of the circular holes. The thickness has been estimated to be 3.0 ± 0.5 nm from our edge-bending method of TEM measurement (see ESI†). From the molecular length of DPC (2.0 nm), it was concluded that the films have a reversed bilayer structure.[17] In the present paper, AFM measurements were conducted for the films covering holes of

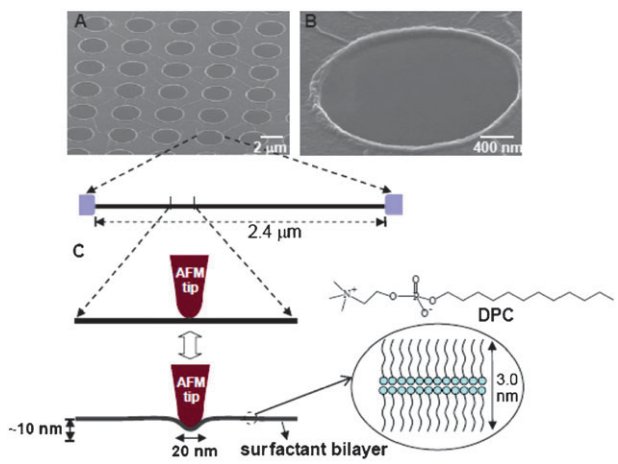

Fig. 1 (a) SEM image of DPC films formed in circular holes of 2.4 μm. (b) Enlarged image of one of the films. QUANTIFOIL® microgrid (Q250-CR2) supplied by Electron Microscopy Sciences was used as substrate. This microgrid has a holey carbon support foil on a 200 mesh copper grid. The nominal thickness of the foil is 12 nm. However, the thickness at the edge of hole was 50 nm, as estimated by SEM observation. (c) Schematic representation of AFM measurements for DFFs in micrometre-sized holes.

[a] *Organic Nanomaterials Center (ONC), National Institute for Materials Science (NIMS), 1-1 Namiki, Tsukuba, Ibaraki 305-0044, Japan. E-mail: Ichinose.Izumi@nims.go.jp; Fax: +81-29-852-7449*
[b] *Research Institute of Biomolecule Metrology, 807-133 Enokido, Tsukuba, Ibaraki 305-0853, Japan*

† Electronic supplementary information (ESI) available: Characterization of DFFs, force–indentation analysis, positioning method of AFM tip, and thermal stability of DFFs. See DOI: 10.1039/b717485c

2.4 μm (or 1.2 μm) in diameter. In the force–displacement measurements, the indentation depth was no more than 30 nm. We used DPC and other three surfactants, dodecyltrimethylammonium bromide (DTAB), octadecyldimethyl(3-trimethoxysilyl-propyl)ammonium chloride (C18NSi) and 1-dodecyl-3-methyl-imidazolium chloride (DMIC). Their thicknesses are 2.5 ± 0.5 nm, 4.7 ± 0.6 nm, and 2.5 ± 0.5 nm, respectively. The scales in the AFM measurements are schematically illustrated in Fig. 1C.

AFM imaging was performed on a Seiko Instruments SPI-4000 microscope in tapping mode in air. We used a silicon nitride cantilever (DNP-S20 from Veeco) at a resonance frequency of 114 kHz. The topographic images of the DPC films are shown in Fig. 2. The films uniformly covered the holes in the carbon foil. The film at the bottom left of Fig. 2A was damaged during the observation. Therefore, the lower two-thirds appeared dark. As shown in Fig. 2B, DPC films were located in each hole at a depth of approximately 35 ± 5 nm from the surface of the carbon foil. The thickness of this foil was about 50 nm, as confirmed by SEM observation. Therefore, DPC films are at a height close to the lower surface. This deviation is probably due to the higher evaporation speed of water at the upper surface. The high magnification image revealed that DPC film was very smooth. The root-mean-square (RMS) roughness was 0.22 nm in an area of 0.5 × 0.5 μm^2 (Fig. 2C). These images were successfully obtained by using a cantilever with a nominal spring constant of 0.06 N m^{-1}. The films were readily damaged, when stiffer cantilevers with a spring constant more than 0.2 N m^{-1} were used. As might be expected, the contact mode was not available at all. We should emphasize here that these are the first examples of AFM imaging of free-standing surfactant bilayers in air.

The nanomechanical properties of surfactant bilayers were examined on an AFM instrument produced by Asylum Research (MFP-3D). The force–displacement curves were obtained in air by using Olympus cantilevers with a spring constant of 0.6–0.7 N m^{-1}. For each cantilever, the spring constant was calibrated by thermal methods.[18] The nominal radius of curvature of the tip was 10 nm. The force and depth resolution was less than 0.02 nN and 0.3 nm, respectively. In the force curve measurements, the approaching and retracting frequency was kept at 0.01 Hz, which corresponded to the speed of 4 nm s^{-1}.

The deflection of the cantilever (d) is generally plotted as a function of the sample displacement (Z).[19,20] If the specimen is stiff, the deflection is proportional to the displacement while the tip contacts the surface of the specimen. On the other hand, soft specimens are readily deformed by the tip when the loading force increases. Then, the indentation (δ) is defined as follows: $\delta = Z - d$. In the real experiments, the offset values, d_0 and Z_0, need to be considered, and the indentation is described as follows: $\delta = (Z - Z_0) - (d - d_0)$, where d_0 is the zero deflection of the cantilever and Z_0 is the contact position. The elastic properties of surfactant bilayers were analyzed with a Hertzian model.[21,22] When the tip has a parabolic shape, the relationship between elastic indentation (δ) and loading force of the cantilever (F) is described as in eqn (1):

$$F = \frac{4}{3}\frac{E}{(1-\nu^2)}\delta^{\frac{3}{2}}\sqrt{R} \qquad (1)$$

where E is Young's modulus, ν is the Poisson ratio (here ν was set to be 0.5), and R is the radius of curvature of the AFM tip (10 nm). The deflection of the cantilever and the loading force are related by Hooke's law ($F = k \times d$). Therefore, we have eqn (2):

$$k(d - d_0) = \frac{4}{3}\frac{E}{(1-\nu^2)}\sqrt{R}[(Z - Z_0) - (d - d_0)]^{3/2} \qquad (2)$$

where k is the spring constant of the cantilever. In our experiments, the Z_0 position was defined as the point with maximum attractive force. Experimentally-obtained

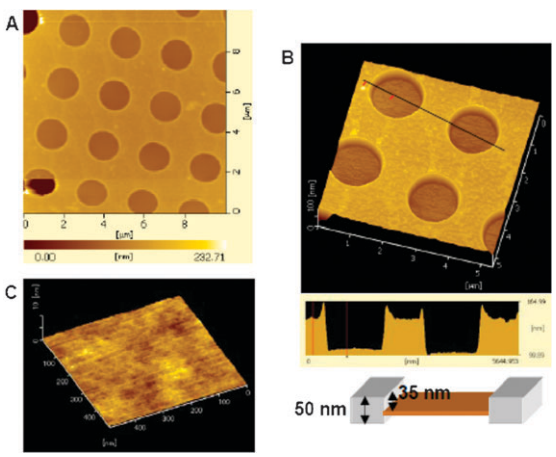

Fig. 2 AFM images of DPC films. (a) Topography image at 10 × 10 μm^2. (b) Topography image at 5 × 5 μm^2 and height profile corresponding to the black line in the image. The location of a DPC film in a hole is shown in a schematic view. (c) High magnification topography image of a DPC film. The substrates were QUANTIFOIL® microgrid (Q250-CR1.3) with holes of 1.2 μm in diameter.

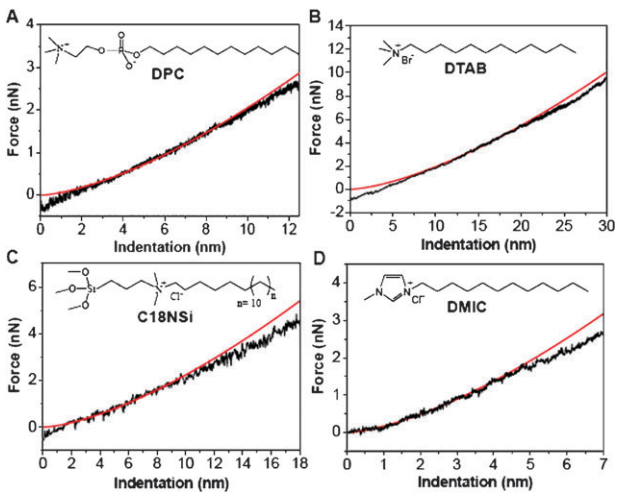

Fig. 3 Force–indentation curves of various DFFs (black lines), their curve fitting by using the Hertzian model (red lines) and structures of surfactant molecules (DPC, DTAB, C18NSi, and DMIC). The force values were adjusted in such a way that the fitting curve gave the minimum value (zero) at the contact point. The substrates were QUANTIFOIL® microgrids with circular holes of 2.4 μm in diameter.

Table 1 Properties of four surfactant molecules and their films

Surfactants	Melting point/°C	DFFs Thickness/nm	Coverage (%)	Thermal stability/°C	Young's modulus/MPa
DPC	265	3.0 ± 0.5	99	150	15.1 ± 3.6
DTAB	246	2.5 ± 0.5	80	150	14.3 ± 3.0
C18NSi	—	4.7 ± 0.6	99	170	12.6 ± 3.5
DMIC	40–43	2.5 ± 0.5	95	90	28.5 ± 5.5

force–indentation curves were fitted with eqn (2) to determine the Young's modulus (E) of surfactant bilayers (see ESI†).

Fig. 3 shows force–indentation curves of four kinds of surfactant bilayers. Each experimental curve was fitted by a Hertzian model. In case of the DPC film, a good curve fitting was not achieved in the indentation range below 3 nm. This indicates that a weak attractive force exists between the film and AFM tip. The curve also gradually deviated from the fitting curve in the indentation range above 9 nm. To verify the adequacy of this curve fitting, we also examined the relationship of the loading force and three-halves power of indentation. Eqn (1) gives a linear relationship between the force (F) and indentation ($\delta^{3/2}$). In fact, the force value in this plot linearly increased in the indentation range of 3–9 nm (see ESI†). The Young's modulus of the DPC films was 15.1 ± 3.6 MPa, as averaged from the values obtained for five force–indentation curves. The fitting curve for the DTAB film slightly deviated in the indentation ranges below 7 nm and above 20 nm. The Young's modulus was estimated to be 14.3 ± 3.0 MPa, which was almost same to that of the DPC film. The behaviour of the C18NSi film was also close to that of the DPC film. The elastic modulus was 12.6 ± 3.5 MPa. On the other hand, the DMIC film gave a relatively large modulus of 28.5 ± 5.5 MPa. The force–indentation curve was in good agreement with the fitting curve for indentations below 5 nm.

The elastic moduli of DFFs are close to those of rubber and are one-tenth to one-hundredth of those of elastic polymers such as polyethylene. DFFs are much stiffer than fluid-like biomembranes. Radmacher summarized that living cells have the elastic modulus of a few 100 Pa up to more than 10 kPa, as determined by a Hertzian model.[20] In sharp contrast, much harder bilayer structures have been reported for a catanionic system that contains cationic and anionic amphiphiles in a specific molar ratio. For example, vesicles formed of myristic acid and cetyltrimethylammonium hydroxide were presumed to have a modulus of 100 MPa or more.[23] In this case, ionic interaction at the two surfaces of the bilayer was deemed to contribute to the stiffness.[24] DFFs with a reversed bilayer structure are slightly softer than the bilayers of this system.

Table 1 summarizes the thickness, and thermal and mechanical properties of DFFs. DPC and DTAB films should have an ionic sheet of hydrophilic head groups between two surfactant monolayers. These films showed thermal stability up to 150 °C and similar nanomechanical properties. The head groups of C18NSi form a two-dimensional siloxane network during the formation of the foam film.[17] Such cross-linking increases the thermal stability up to 170 °C and contributes to the film strength. However, the Young's modulus slightly decreased as compared with the above two surfactant molecules. Interestingly, the stiffest film was obtained from DMIC. This surfactant has a methylimidazolium head group, which is familiar as a moiety of ionic liquids. Despite the low melting point of about 40 to 43 °C, the reversed bilayer structure was stable up to 90 °C and gave the highest Young's modulus of 28.5 MPa. The reasons for this stiffness are not very clear so far. However, the molecular interaction of DMIC in the bilayer must be stronger than that of the other surfactant. In addition, the high thermal stability indicates the existence of two-dimensional ionic sheets similar to the cases of DPC and DTAB.

We demonstrated that the elastic moduli of DFFs are quite high, as compared with those of biomembranes. Although the ultimate strength of these surfactant bilayers has been unclear due to technical limitations, the present results will contribute to the understanding of molecularly thin organic films suspended in air.

Notes and references

1. E. W. Wong, P. E. Sheehan and C. M. Lieber, *Science*, 1997, **277**, 1971.
2. S. Cuenot, S. Demoustier-Champagne and B. Nysten, *Phys. Rev. Lett.*, 2000, **85**, 1690.
3. A. Heidelberg, L. T. Ngo, B. Wu, M. A. Phillips, S. Sharma, T. I. Kamins, J. E. Sader and J. J. Boland, *Nano Lett.*, 2006, **6**, 1101.
4. J. S. Bunch, A. M. Van der Zande, S. S. Verbridge, I. W. Frank, D. M. Tanenbaum, J. M. Parpia, H. G. Craighead and P. L. McEuen, *Science*, 2007, **315**, 490.
5. S. S. Ono and G. Decher, *Nano Lett.*, 2006, **6**, 592.
6. T. C. Merkel, B. D. Freeman, R. J. Spontak, Z. He, I. Pinnau, P. Meakin and A. J. Hill, *Science*, 2002, **296**, 519.
7. D. M. Sullivan and M. L. Bruening, *Chem. Mater.*, 2003, **15**, 281.
8. R. Vendamme, S.-Y. Onoue, A. Nakao and T. Kunitake, *Nat. Mater.*, 2006, **5**, 494.
9. P. A. O'Connell and G. B. McKenna, *Science*, 2005, **307**, 1760.
10. W. A. Goedel and R. Heger, *Langmuir*, 1998, **14**, 3470.
11. S. Markutsya, C. Jiang, Y. Pikus and V. V. Tsukruk, *Adv. Funct. Mater.*, 2005, **15**, 771.
12. A. A. Mamedov, N. A. Kotov, M. Prato, D. M. Guldi, J. P. Wicksted and A. Hirsch, *Nat. Mater.*, 2002, **1**, 190.
13. A. Kovalev, H. Shulha, M. Lemieux, N. Myshkin and V. V. Tsukruk, *J. Mater. Res.*, 2004, **19**, 716.
14. S. A. Chizhik, Z. Huang, V. V. Gorbunov, N. K. Myshkin and V. V. Tsukruk, *Langmuir*, 1998, **14**, 2606.
15. J. Heuvingh, M. Zappa and A. Fery, *Langmuir*, 2005, **21**, 3165.
16. K. E. Mueggenburg, X.-M. Lin, R. H. Goldsmith and H. M. Jaeger, *Nat. Mater.*, 2007, **6**, 656.
17. (*a*) J. Jin, J. Huang and I. Ichinose, *Angew. Chem., Int. Ed.*, 2005, **44**, 4532; (*b*) J. Jin, Y. Wakayama, X. Peng and I. Ichinose, *Nat. Mater.*, 2007, **6**, 686.
18. J. L. Hutter and J. Bechhoefer, *Rev. Sci. Instrum.*, 1993, **64**, 1868.
19. N. J. Tao, S. M. Lindsay and S. Lees, *Biophys. J.*, 1992, **63**, 1165.
20. M. Radmacher, *Method Cell Biol.*, 2002, **68**, 67.
21. H. Hertz, *J. Reine Angew. Math.*, 1882, **92**, 156.
22. I. N. Sneddon, *Int. J. Eng. Sci.*, 1965, **3**, 47.
23. M. Dubois, B. Demé, T. Gulik-Krzywicki, J.-C. Dedieu, C. Vautrin, S. Désert, E. Perez and T. Zemb, *Nature*, 2001, **411**, 672.
24. M. A. Hartmann, R. Weinkamer, T. Zemb, F. D. Fischer and P. Fratzl, *Phys. Rev. Lett.*, 2006, **97**, 018106.

